Dev Genes Evol (2008) 218:453–463
DOI 10.1007/s00427-008-0236-x

ORIGINAL ARTICLE

Vasa and *nanos* are coexpressed in somatic and germ line tissue from early embryonic cleavage stages through adulthood in the polychaete *Capitella* sp. I

Kariena K. Dill · Elaine C. Seaver

Received: 7 April 2008 / Accepted: 16 June 2008 / Published online: 24 July 2008

Abstract Members of the *vasa* and *nanos* gene families are involved in germ line development in a number of diverse animals. As a polychaete annelid model for studies of the germ line, *Capitella* sp. I has several advantages including the presence of dedicated gonads, individuals that reproduce multiple times, and the presence of males, females, and hermaphrodites. Germ line development has not been characterized in *Capitella* sp. I, nor is the mechanism of germ line specification generally well understood in annelids. We have cloned *vasa* and *nanos* orthologues from *Capitella* sp. I and found that both *CapI-vasa* and *CapI-nanos* transcripts are expressed in developing gametes of sexually mature adults. Characterization of both these genes during embryonic, larval, and juveniles stages reveals expression in multiple somatic tissues for *CapI-vasa* and *CapI-nanos* with largely overlapping but not identical expression patterns. In early cleavage stages, both transcripts are broadly expressed; following gastrulation, expression is observed in the presumptive brain, mesodermal bands, and developing foregut. Using *CapI-nanos* and *CapI-vasa* as markers, we have identified putative primordial germ cells (PGCs) in larvae, which are initially present as small bilateral clusters in segment 4 and as a single cluster at late larval stages. In adults, a single large cluster of putative PGCs is present in segments 5 and 6. In addition to highlighting differences in expression profiles for these two genes among lophotrochozoans, we present a hypothesis concerning the origin and development of PGCs in *Capitella* sp. I.

Communicated by D.A. Weisblat

K. K. Dill · E. C. Seaver (✉)
Kewalo Marine Laboratory, Pacific Biosciences Research Center,
University of Hawaii,
41 Ahui Street,
Honolulu, HI 96813, USA
e-mail: seaver@hawaii.edu

Keywords Spiralia · Vasa · Nanos · Primordial germ cell · Germ line

Introduction

In sexually reproducing animals, development of a viable germ line is essential for reproductive success and survival of the species. In most species, the germ line has a single embryonic origin, the primordial germ cells (PGCs), which are defined as a population of undifferentiated stem cells that will exclusively give rise to germ cells (Extavour and Akam 2003). Two very different mechanisms of PGC specification have been identified among metazoan species. In some animals, including *Drosophila* (Williamson and Lehmann 1996), *C. elegans* (Kimble and White 1981), and zebrafish (Yoon et al. 1997), PGCs are specified early in development by maternally inherited cytoplasmic determinants (preformation). In other animals, including mouse (Lawson and Hage 1994; Tam and Zhou 1996) and axolotl (Nieuwkoop 1947), PGCs are specified later in development by inductive signals from neighboring tissues (epigenesis). Among metazoans, epigenesis is more prevalent than preformation and is also the mechanism found in basal metazoans (e.g., cnidarians and sponges; reviewed in Extavour and Akam 2003). For these reasons, epigenesis is proposed to be the ancestral mode of germ cell specification in the Metazoa.

Studies in model organisms indicate that, regardless of whether a species exhibits preformation or epigenesis, at least some aspects of the molecular patterning of germ line development are well conserved. The Vasa and Nanos gene products are expressed in PGCs in nearly every species examined and have been shown to regulate germ line development in a variety of species (reviewed in Extavour and Akam 2003). Vasa-related proteins are adenosine triphosphate-dependent

ribonucleic acid (RNA) helicases and members of the DEAD box protein family (Mochizuki et al. 2001). Numerous studies suggest that *vasa* genes are expressed exclusively in potential germ cell progenitors or other stem cells (Extavour and Akam 2003). However, recent reports for a polychaete (*Platynereis dumerilii*) have identified *vasa* expression in the germ line as well as in multiple somatic tissues, including the mesodermal bands, brain, foregut, and posterior growth zone (Rebscher et al. 2007; Zelada-González 2005). Likewise, in the oligochaete annelid, *Tubifex tubifex*, *vasa* is broadly expressed during cleavage stages and in the presumptive segmental tissues in addition to the germ line (Oyama and Shimizu 2007).

Nanos proteins contain two highly conserved CCHC zinc fingers in the C terminus with little conservation outside of this domain (Curtis et al. 1997). Nanos family proteins function as translational inhibitors (Curtis et al. 1997) and regulate both somatic and germ line development (reviewed in Extavour and Akam 2003). Among lophotrochozoans, *nanos*-related genes are expressed in the germ line in *Helobdella robusta* (a leech; Kang et al. 2002) and in PGCs in *P. dumerilii* (a polychaete) (Rebscher et al. 2007; Zelada-González 2005). These and other lophotrochozoan studies also report *nanos* expression in somatic tissues. *H. robusta nanos* is expressed in ectodermal stem cells (Kang et al. 2002), and *P. dumerilii nanos* is expressed in multiple somatic tissues including brain, foregut, and mesodermal bands (Zelada-González 2005). The *Ilyanassa obsoleta* (a snail) *nanos* gene becomes restricted to the 4d mesoderm lineage, and morpholino knockdown of *nanos* results in loss of mesodermal and endodermal tissues (Rabinowitz et al. 2008).

This study examines *vasa*- and *nanos*-related genes in *Capitella* sp. I, a member of the phylum Annelida. *Capitella* sp. I is a benthic marine polychaete with male, female, and hermaphrodite sexes. In females, oocytes develop in paired ovaries attached to the body wall in mid-body segments (Eckelbarger 1984). Sperm development takes place in paired sac-like genital ducts suspended in the lateral coelom between the seventh and eighth segments (Eckelbarger and Grassle 1987a). Oogenesis and spermatogenesis have been studied in young adults (Eckelbarger and Grassle 1983, 1987b; Eckelbarger et al. 1984); however, germ line development has not been examined during embryonic or larval stages. PGCs have not yet been identified, and the mechanism of germ line specification (preformation or epigenesis) is unknown. Furthermore, germ cell differentiation can be labile in *Capitella* sp. I: (1) Adult males can transform into fertile hermaphrodites (Holbrook and Grassle 1984), and (2) adult females can regenerate segments with ovaries (Hill, personal communication). Although these phenomena suggest an epigenetic mechanism of germ line development, germ line regulation in adults may involve a mechanism distinct from that involved in embryonic or larval development. For example, in the ascidian *Ciona intestinalis*, PGCs are localized to the tail of the tadpole stage, which migrate into the adult gonad rudiment during metamorphosis. If the tail and PGCs are removed, resulting in adults forming mature sperm, suggesting that in ascidians, there is a compensatory mechanism that regulates germ line formation at a later life history stage (Takamura et al. 2002). To begin to investigate the embryonic origin(s) of PGCs and the primary mode of germ line development in *Capitella* sp. I, we isolated orthologs of the *vasa* (*CapI-vasa*) and *nanos* (*CapI-nanos*) gene families and examined their developmental expression patterns by whole-mount in situ hybridization during embryonic, larval, juvenile, and adult stages.

Materials and methods

Cloning of *Capitella* sp. I *vasa* and *nanos* genes

Several overlapping expressed sequence tag (EST) sequences representing a single *nanos* homolog (*CapI-nanos*) and another set representing a single *vasa* homolog (*CapI-vasa*) were identified in BLAST searches of *Capitella* EST libraries (sequenced by the Joint Genome Institute [Department of Energy, Walnut Creek, CA, USA] as part of the *Capitella* sp. I 8x genome sequencing project). Each set of sequences was aligned and compiled into a single predicted transcript for each gene. The predicted transcripts were submitted to National Center for Biotechnology Information (NCBI) as third-party annotation sequences with the following accession numbers: *CapI-nanos* (BK006522) and *CapI-vasa* (BK006523). Two ESTs representing *CapI-nanos* were recovered from glycerol stocks of a pBluescript SK phagemid (Stratagene) mixed-stage complementary deoxyribonucleic acid (cDNA) library and sequenced (Macrogen, Seoul, South Korea) for verification; clone 4923 contains a 2,067-bp fragment corresponding to base pairs 267–2,334 of the full-length transcript, and clone 16516 contains an 812-bp fragment representing base pairs 800–1,612. Sequence of the *CapI-vasa* EST was used to design primers (forward: 5′-GTGTGGTGAAGAAGGGCATT-3′; reverse: 5′-GGGAACTCGGACTGAGACAA-3′) to amplify this sequence from *Capitella* cDNA. The resulting 1,122-bp fragment was ligated into pGEM T-easy vector (Promega) and sequenced.

Phylogenetic analysis

Phylogenetic analyses of the Nanos and Vasa families were performed to determine gene orthology. We assembled sets of Nanos and Vasa protein sequences from multiple species representing diverse metazoan taxa. Amino acid alignments were made with the ClustalW program included in the MacVector package. Analysis of the Nanos protein sequences

was carried out with MrBayes 3.1.2 (Ronquist and Huelsenbeck 2003) using the "wag" amino acid model and 10^6 generations sampled every 100 generations with four chains over a single run. Neighbor-joining analysis was performing using PAUP*4.0b10 (Swofford, 2002) with 1,000 replicates. Analysis of the Vasa family was carried out using an amino acid alignment of the DEAD-box domains from the following sequences: *H. robusta* predicted Vasa-like protein (HroVasa), JGI protein ID: 65423; *I. obsoleta* Vasa (IoVasa), ABU49329; *Capitella* sp. I predicted PL10-like protein (CapIPL10, JGI protein ID: 224610; *Capitella* sp. I Vasa, BK006523; *Lottia gigantea* predicted Vasa-like protein (LgVasa), JGI protein ID: 177322; *P. dumerilii* PL10a (PdPL10a), CAJ15140; *P. dumerilii* PL10b (PdPL10b), CAJ15141; *P. dumerilii* Vasa (PdVasa), CAJ38803; *Strongylocentrotus purpuratus* Vasa (SpVasa), XP_781494; *Ephydatia fluviatilis* Vasa (EfVasa), BAB13310; *E. fluviatilis* PL10-related protein (EfPL10), BAB13309; *Mus musculus* Ddx4 (MmVasa), EDL18409; *M. musculus* PL10 (MmPL10), NP_149068; *Crepidula fornicata* PL10 (CfPL10), ABD59346; *Danio rerio* PL10 (DrPL10), NP_571016; *D. rerio* Vasa (DrVasa), NP_571132; *Nematostella vectensis* PL10 (NvPL10), AAW29072; *N. vectensis* Vasa2 (NvVasa2), AAW29074; *N. vectensis* Vasa1 (NvVasa1), AAW29073; *C. intestinalis* Vasa (CiVasa), BAA36710; *Enchytraeus japonensis* Vasa (EjVasa), BAF76795; *Crassostrea gigas* Vasa (CgVasa), AAR37337; *Hydra magnipapillata* Vasa (HmVasa), BAB13307. Analysis of the Nanos family was carried out using an amino acid alignment of the two CCHC zinc finger domains from the following sequences: *I. obsoleta* Nanos (IoNos), ABV54788; *H. robusta* Nanos (HroNos), AAB63111; *Podocoryne carnea* Nanos (PcNos), AAU11514; *H. magnipapillata* Nanos2 (HmNos2), BAB01492; *M. musculus* Nanos (MmNos), NP_848508; *N. vectensis* Nanos2 (NvNos2), AAW29071; *N. vectensis* Nanos1 (NvNos1), AAW29070; *Apis mellifera* Nanos (AmNos), NP_001035321; *D. rerio* Nanos (DrNos), AAH97090; *L. gigantea* predicted Nanos protein (LgNos), JGI protein ID: 60286; *P. dumerilii* Nanos (PdNos), CAJ28985; *Capitella* sp. I Nanos (CapINos), BK006522; *Drosophila melanogaster* Nanos (DmNos), AAA28715; *Schistocerca americana* Nanos (Sa), AAO38523; *T. tubifex* Nanos (TtNos), BAD90110; *Xenopus tropicalis* Nanos (XtNos), NP_988857; *Drosophila simulans* Nanos (DsNos), AAF68510; *Caenorhabditis elegans* Nanos2 (CeNos2), AAB93424; *Caenorhabditis elegans* Nanos1 (CeNos1), NP_496358; *E. fluviatilis* Nanos (EfNos), BAB19253; *Musca domestica* Nanos (MdNos), AAA87461; *Chironomus samoensis* Nanos (CsNos), AAA87459; *Xenopus laevis* Xcat2 (XlXcat2), NP_001081503; *Anopheles gambiae* Nanos (AgNos), AAW71999; *Homo sapiens* Nanos1 (HsNos), NP_955631. JGI predicted protein sequences were obtained from the Joint Genome Institute web browsers for each species (http://genome.jgi-psf.org/); all other accession numbers were obtained from NCBI.

Animal husbandry and in situ hybridization

A *Capitella* sp. I colony was maintained in the laboratory using published culture methods (Grassle and Grassle 1976) and broods were recovered as described previously (Seaver et al. 2005). Embryos and larvae were dissected from brood tubes, fixed in 3.7% formaldehyde in filtered sea water at 4°C for 16–24 h and then processed for whole-mount in situ hybridization according to published protocols (Seaver and Kaneshige 2006; Seaver et al. 2001). Juveniles and adults were treated with the same conditions as embryos and larvae with the exception that proteinase K treatment was increased from 3 to 10 (juveniles) or 20 min (adults), and for adult stage in situ experiments, the volume of all washes and hybridizations was increased from 0.5 to 1 ml. Digoxigenin-labeled riboprobes were generated with the MEGAscript kit (Ambion); following hybridization, probes were detecting using nitroblue tetrazolium chloride/5-bromo-4-chloro-3-indolyphosphate color substrate. Riboprobes were generated for two ESTs representing fragments of *CapI-nanos* (16516 and 4923) and one clone representing a fragment of *CapI-vasa* (see above). The two *nanos* probes gave identical results at all stages examined; embryos shown in Fig. 2 were hybridized with riboprobe generated from EST 16516.

Results and discussion

Cloning and phylogenetic analyses of *Capitella* sp. I *nanos* and *vasa* genes

Searches of the *Capitella* sp. I genome identified a single *nanos*-related gene and ESTs representing this *nanos*-related gene were identified with BLASTX searches of sequenced EST libraries (see "Materials and methods"). The full-length *CapI-nanos* transcript is predicted to encode a 327-amino acid protein, which includes two CCHC zinc finger domains that display a high degree of amino acid identity with other metazoan Nanos proteins. Phylogenetic analysis based on an amino acid alignment of the two CCHC zinc finger domains of Nanos proteins from a diverse representation of metazoan species confirms *CapI-nanos* as a member of the Nanos gene family (Fig. 1a). CapI-Nos groups with other lophotrochozoan Nanos proteins and is more closely related to vertebrate, cnidarian, and arthropod sequences than to the *C. elegans* Nanos proteins (Fig. 1a), which form an outgroup in this and previous analyses of the Nanos family (Extavour et al. 2005). No additional *nanos*-related genes were identified in our searches of the *Capitella* sp. I genome, consistent with the presence of a single *Capitella nanos* gene.

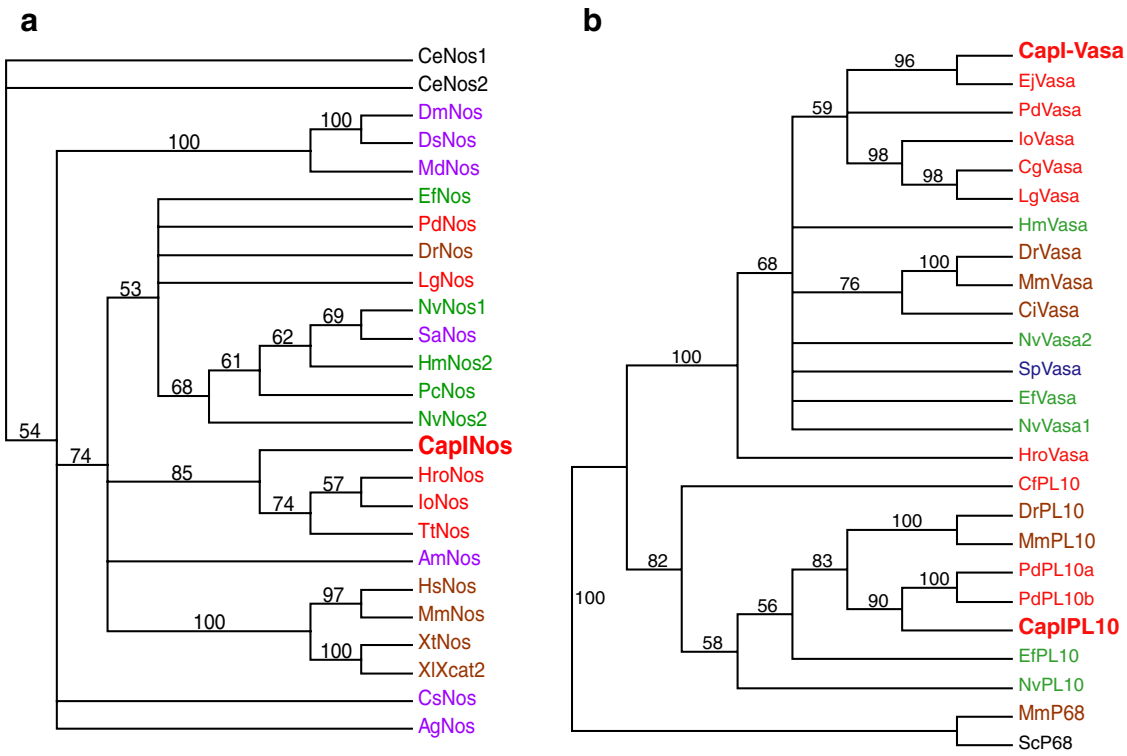

Fig. 1 Phylogenetic analysis of *Capitella* sp. I vasa and nanos genes. Color-coding for both trees is as follows: *red*=lophotrochozoan, *violet*=arthropod, *green*=cnidarian and sponge, *brown*=chordate, *black*=nematode, and *blue*=echinoderm. **a** Bayesian consensus tree of the CCHC zinc finger domains of metazoan nanos genes. Numbers above branches indicate posterior probabilities. **b** Neighbor-joining consensus tree depicting the relationship among DEAD-box helicase domains of metazoan *vasa* and *PL10* genes. Numbers above the horizontal branches indicate bootstrap values for neighbor-joining analysis. Species abbreviations are as indicated in "Materials and methods"

Sequence searches of the *Capitella* sp. I genome identified a single *vasa* gene, *CapI-vasa*. The *CapI-vasa* transcript is predicted to encode a protein of 515 amino acid residues (CapI-Vasa) containing a conserved DEAD-box helicase domain. This domain is characteristic of genes in the DEAD-box protein family, which includes the closely related Vasa and PL10 subfamilies (Mochizuki et al. 2001). The amino acid sequence of CapI-Vasa is most closely related to other Vasa-related proteins. We performed a phylogenetic analysis of the helicase domains from *Capitella vasa* and *PL10* genes to determine the orthology of *CapI-vasa*. The analysis confirms an orthology assignment of *CapI-vasa* as a member the Vasa family (Fig. 1b). *CapI-vasa* clusters with *vasa* genes from other species with a strong bootstrap support value (100), while *CapI-PL10*, an additional DEAD-box gene identified in *Capitella* sp. I genomic sequences, clusters with the *PL10* genes (Fig. 1b). Within the Vasa cluster, CapI-Vasa is most similar to a sequence from an oligochaete (EjVasa), and also groups with Vasa orthologues from other lophotrochozoans (Fig. 1b).

CapI-nanos mRNA embryonic, larval, and juvenile expression patterns

CapI-nanos transcript is detected in the yolk-free cytoplasm surrounding the nucleus in uncleaved zygotes (Fig. 2a). This pattern indicates maternal expression but does not suggest specific asymmetric localization. Through early cleavage stages, *CapI-nanos* is broadly expressed in most if not all cells (including all four embryonic quadrants) and co-localizes with the nuclei (Fig. 2b,c). At the 56-cell stage (fifth to sixth cleavage), expression is enriched in 4d daughter cells (Fig. 2c, arrows), although it is also detected at lower levels throughout the embryo. This pattern contrasts with the restricted messenger RNA (mRNA) expression for a *nanos* gene at a similar stage in the snail, *I. obsoleta* (Rabinowitz et al. 2008). Although *nanos* is expressed broadly during early cleavage in this lophotochozoan species, after fourth-quartet micromeres are born, expression becomes highly restricted to the 4d lineage (Rabinowitz et al. 2008). In the *Helobdella* embryo (leech), Nanos protein is robustly expressed in ectodermal precursor cells during cleavage with lower expression levels in mesodermal precursors. Thus, leech *nanos* also lacks restricted expression in the 4d lineage (Pilon and Weisblat 1997).

At the end of gastrulation (stage 3), *CapI-nanos* expression transitions to a more discrete pattern with four distinct domains (Fig. 2d–g) that includes the presumptive brain (Fig. 2f), the closing blastopore (Fig. 2d), a pair of cells straddling the dorsal midline (Fig. 2g), and mesodermal cells (Fig. 2d,e). In the following section, we elaborate on the

details of expression for each of these domains individually as they progress through larval development.

CapI-nanos is expressed in two bilateral patches of anterior ectoderm during stages 3 and 4 (Fig. 2f,h). This expression domain corresponds to the presumptive brain (Meyer and Seaver, in preparation). By stage 6, when the brain is morphologically distinct from the overlying ectoderm, *CapI-nanos* is expressed in the brain (Fig. 2l,n). Expression in the brain is reduced by stage 8 (Fig. 2o) and is not detected at later developmental stages.

CapI-nanos transcript is detected in the foregut at very early stages of foregut development (stage 4; Fig. 2i) in cells that likely correspond to at least a subset of the *CapI-nanos*-positive cells around the closing blastopore at stage 3 (Fig. 2d). Robust foregut expression is detected at mid-larval stages (e.g., stage 6, Fig. 2l, n) and at low levels at stage 8 (Fig. 2o). *CapI-nanos* is also briefly expressed in the hindgut during stages 5–6 (Fig. 2l,n, and data not shown).

A line of *CapI-nanos*-positive cells are also apparent immediately anterior to the telotroch (Fig. 2j, k)—the posterior larval ciliary band—at stage 4, in a similar position to the dorsal *CapI-nanos*-expressing cells at stage 3 (Fig. 2g). These *CapI-nanos*-positive cells are large ectodermal cells that form a band around most of the circumference of the larva, although no expressing cells span the ventral midline. The position of this band of cells corresponds with the future posterior growth zone, and these cells may represent ectoteloblasts. Within each cell, the transcript is localized to the nucleus (Fig. 2k), and the most prominent expression is restricted to a small spot within the nucleus. There are no unlabeled ectodermal cells interspersed between the *CapI-nanos*-positive cells that make up this band (Fig. 2k), and expression of *CapI-nanos* in these cells is not detected at any later stages of development.

In spiralians (including molluscs and annelids), the germ line is assumed to be of mesodermal origin arising from the 4d lineage (Extavour and Akam 2003). *CapI-nanos* expression in the 4d descendants (Fig. 2d,e) may encompass cells that will give rise to the germ line; however, it is clearly not exclusive to the germ line, as the major derivative of these cells is segmental mesoderm, which includes body wall and visceral muscle and coelomic cavity linings. The mesoderm precursor cells (and their derivatives) continue to divide during stage 3 such that by stage 4, they have formed two bilateral bands (the mesodermal bands), which expand circumferentially around the larva, generating the mesodermal component of the first ten segments (Seaver et al. 2005). *CapI-nanos* is expressed throughout the mesodermal bands at stage 4 (Fig. 2i,j). At stage 6, *CapI-nanos* is broadly expressed in the segmental region (between the prototroch and telotroch) with strongest expression in the posteriormost segments (Fig. 2l,n). In lateral view, it is apparent that the segmental *CapI-nanos* expression encompasses both mesodermal and ectodermal tissues; expression abuts the yolky endoderm and extends outward to the surface of the ectoderm (Fig. 2n). After stage 6, expression diminishes in the formed segments, and robust expression is maintained in the posterior growth zone at late larval (Fig. 2o,p,t) and juvenile stages (Fig. 2u,v).

At stage 6, an additional *CapI-nanos* expression domain appears, in two bilateral ventro-lateral clusters of cells in segment 4 (Fig. 2m). This expression domain is more easily detected at stage 8, when the overlying mesoderm and ectoderm expression has diminished (Fig. 2o,p,q). There are no previous descriptions of any structure(s) that develop at the position of these *CapI-nanos*-positive cells. Because of the morphology of these cells and the fact that *CapI-vasa* is also expressed in this region (see below), we consider them as putative PGCs. Within segment 4, three distinct patterns of *CapI-nanos* PGC expression are observed among stage 8 larvae: (1) two bilaterally symmetric cell clusters (Fig. 2p, q, $n=6$), (2) two asymmetrically positioned clusters at or near the midline (Fig. 2r, $n=8$), and (3) a single cluster centered on the midline (Fig. 2s, $n=14$). These three different patterns of *CapI-nanos* PGC expression may indicate that the two ventro-lateral clusters migrate to the midline during stage 8. Alternatively, one of the clusters may be developmentally lost. From our expression data, it is not possible to distinguish between these two alternatives. Viewing the PGCs at 100× magnification shows perinuclear localization of the *CapI-nanos* transcript and large nuclear to cytoplasmic ratio (Fig. 2q). By stage 9, *CapI-nanos* expression is dramatically reduced and is only detected in a single PGC cluster at the midline and in the mesoderm and ectoderm of the posterior growth zone (Fig. 2t). There is no evidence of *CapI-nanos* expression in PGCs in juvenile stages.

CapI-vasa mRNA embryonic, larval, and juvenile expression patterns

With a few exceptions, *CapI-vasa* mRNA expression overlaps with that of *CapI-nanos* throughout all stages examined. Like *CapI-nanos*, *CapI-vasa* transcript is maternally expressed and appears in the yolk-free cytoplasm surrounding the nucleus in the uncleaved zygote (Fig. 3a). Expression is detected throughout cleavage in most if not all cells (Fig. 3b,c). Although we could not find any *CapI-vasa*-negative cells, it is possible that a nonexpressing cell went undetected. At 56-cell stage, *CapI-vasa* expression appears in the cytoplasm and the nuclei of most cells, but in some cells, it appears to be localized to the nucleus (Fig. 3b,c). In contrast to *CapI-nanos* expression at the 56-cell stage (Fig. 2c), *CapI-vasa* expression does not appear to be enriched in 4d derivatives (Fig. 3c). A study from *I. obsoleta* reports *vasa* transcript expression limited to a subset of 4d derivatives during cleavage and no expression detected at

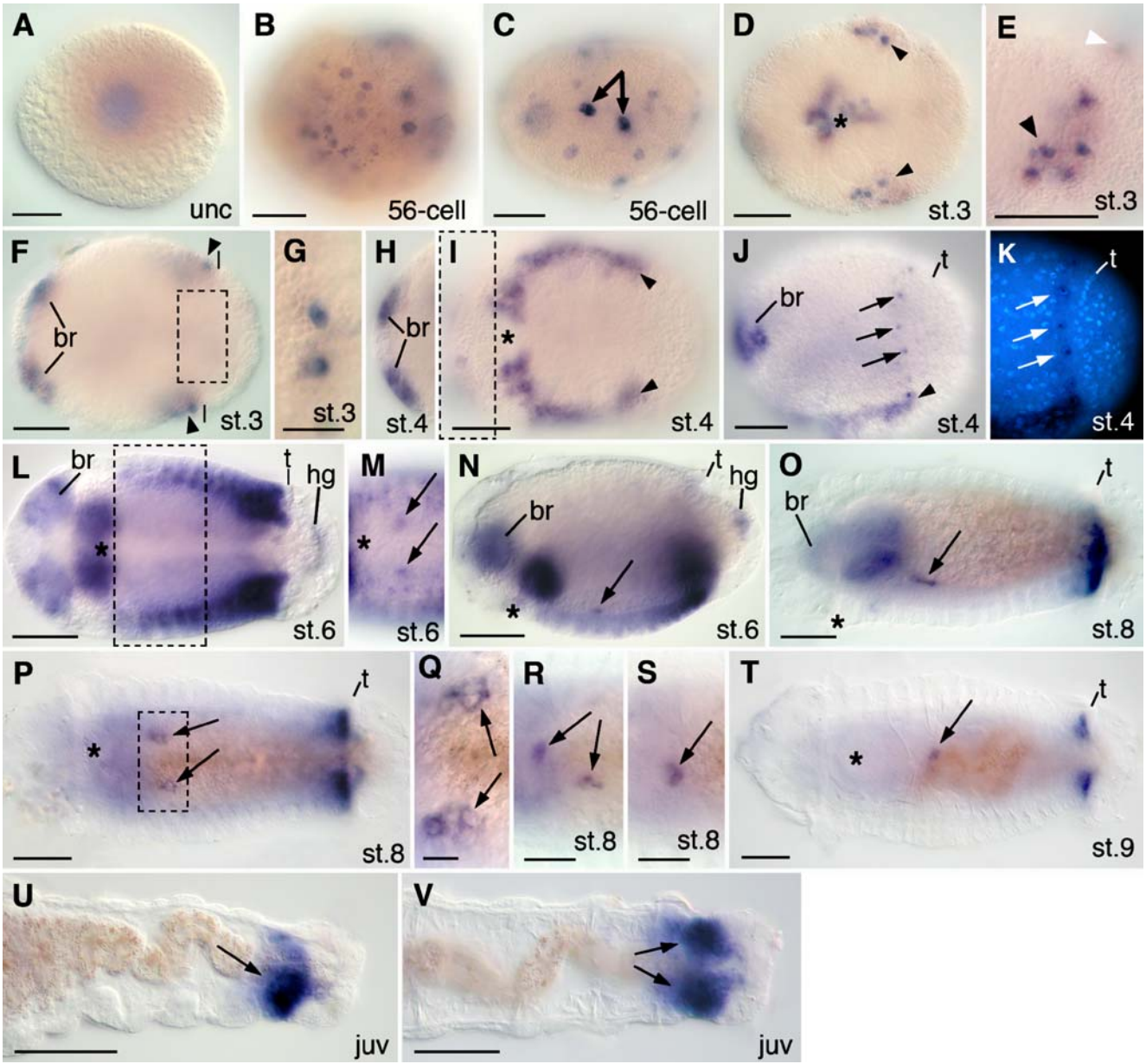

any later stage (Swartz et al., 2008). Thus, *CapI-vasa* expression does not correlate with the expression reported in this mollusc.

At stage 3, *CapI-vasa* is detected in three of the four *CapI-nanos* expression domains: in the presumptive brain (Fig. 3f), around the closing blastopore (Fig. 3d), and in the region of 4d mesodermal descendants (Fig. 3d–f). In contrast to the nuclear localization of *CapI-nanos* in these three domains at stage 3 (Fig. 2d–g), the *CapI-vasa* transcript is present in the cytoplasm. Posterior to the mesodermal expression domain, a few surface cells show nuclear *CapI-vasa* expression (Fig. 3d). These cells do not show any particular arrangement and may represent residual expression from cleavage stages. At stage 4, *CapI-vasa* is detected in the brain (Fig. 3g), in the presumptive foregut (Fig. 3h), and in the mesodermal bands (Fig. 3h, i). In contrast to *CapI-nanos* (Fig. 2j, k), no *CapI-vasa* expression was detected in the row of ectodermal cells anterior to the telotroch (Fig. 3i). Throughout the rest of larval development, *CapI-vasa* expression is nearly indistinguishable from *CapI-nanos* expression. *CapI-vasa* mRNA is detected in the developing brain (Fig. 3j–l), foregut (Fig. 3j,k,m), hindgut (Fig. 3k), and in the segmental mesoderm (Fig. 3j,k,m). At stage 6, expression is detected throughout the segmental mesoderm (Fig. 3j inset) with strong expression in both the ectoderm and mesoderm of posterior segments (Fig. 3k). Segmental expression begins to diminish at stage 7 and becomes highly reduced except for strong expression in the posterior growth zone at stages 8 (Fig. 3l, m) and 9 (Fig. 3q). In juveniles, CapI-vasa is expressed in the ectoderm and mesoderm of the

Fig. 2 *CapI-nanos* RNA expression patterns during embryonic, larval, and juvenile development. The image in panel **q** was captured using a 100× objective, all other images were taken with a 40× objective. Except for cleavage stages (**a**–**c**), all animals are oriented anterior to the left. In lateral views, ventral is down. An *asterisk* marks the position of the blastopore (stage 3) or stomodeum (stages 4–9), *t* indicates the telotroch, and *br* indicates the brain in all panels. **a** In the uncleaved zygote, *CapI-nanos* RNA is detected in the yolk-free cytoplasm. **b** Animal view at the 56-cell stage shows nuclear expression of *CapI-nanos* throughout the embryo. **c** An equatorial view (vegetal down) facing the D-quadrant at the 56-cell stage shows *CapI-nanos* expression in all nuclei in view; expression appears enriched in the 4d daughter cells (*arrows*). **d** Ventral view of a late gastrula embryo (stage 3). *CapI-nanos* expression colocalizes with the nucleus in cells around the closing blastopore (*asterisk*) and in two ventro-lateral cell clusters (*arrowheads*), in the position of 4d derived mesodermal cells. **e** shows a lateral close-up of *CapI-nanos* expression in the mesoderm stem cells (*black arrowheads*, refers to region denoted by *black arrowheads* in **d**). *White arrowhead* points to one of the dorsal cells shown in **g**. **f** Dorsal view shows *CapI-nanos* expression in the presumptive brain and in the mesoderm stem cells (*arrowheads*). The position of the presumptive telotroch is marked by *vertical lines*. **g** Enlarged view in a more surface focal plane of the *boxed region* shown in **f** highlighting two additional *CapI-nanos*-positive cells flanking the dorsal midline. **h**, **i**, **j** *CapI-nanos* expression in the brain (**h**, **j**), foregut (staining lateral to the stomodeum in **i**), and in the mesodermal bands (**i**, *arrowheads*) in ventral (**h**, **i**) and lateral (**j**) views. *Boxed area* in **i** denotes position of view depicted in (**h**) at a different focal plane. **j**, **k** Same stage 4 embryo with a DIC image (**j**) and a Hoechst 33342 stain (**k**) showing *CapI-nanos*-positive ectodermal cells (*arrows*) positioned in a circumferential row immediately anterior to the telotroch (*t*). **l** Ventral and **n** lateral views of a stage 6 larva showing continued *CapI-nanos* expression in the brain (*br*) and foregut (staining lateral and dorsal to the stomodeum), expanded expression in the body segments (between the stomodeum and telotroch), and in a small domain in the hindgut (*hg*). **m**, **n** Two ventro-lateral clusters of *CapI-nanos*-expressing cells are located in segment 4 (*arrows*), positioned between the yolky endoderm and the ventral nerve cord (putative primary germ cells, PGCs). Image in **m** is a cropped view of a ventral focal plane centered around region depicted by *box* in **l**. Lateral (**o**) and ventral (**p**) views of stage 8 larvae show strong *CapI-nanos* expression in the PGCs (*arrows*) and posterior growth zone (staining anterior to the telotroch); low levels of expression are also detected in the brain, foregut, and body segments. *Box* in **p** depicts region shown in **q**, **r**, and **s**. **q** The PGCs in **p** were viewed at 100× magnification to highlight the perinuclear pattern of *CapI-nanos* staining in these cells. Three distinct patterns of *CapI-nanos* PGC expression are observed among stage 8 larvae: two bilaterally symmetrical cell clusters (**p**, **q**), two clusters positioned asymmetrically at or near the midline (**r**), and a single cluster centered on the midline (**s**) (ventral views). **t** By stage 9, *CapI-nanos* expression is limited to a single PGC cluster at the midline (*arrow*) and mesoderm and ectoderm of the posterior growth zone. **u**, **v** During early juvenile stages (*juv*), *CapI-nanos* is expressed exclusively in the ectoderm and mesoderm of the posterior growth zone (*arrows*; posterior end, **u**, lateral view; **v**, ventral view). Note mesodermal expression that extends posterior into the pygidium. *Scale bar*, 50 μm for all panels except **g**, **q**, **r**, and **s**. *Scale bar* in **g**, 20 μm; *scale bar* in **q**, 10 μm; *scale bar* in **r** and **s**, 25 μm

posterior growth zone and weakly in the ventral nerve cord (Fig. 3r,s).

At stages 6 and 7, *CapI-vasa* expression is detected in two ventro-lateral clusters of cells in segment 4, the PGCs (Fig. 3j, k, and not shown for St. 7). As described for *CapI-nanos*, three different patterns of *CapI-vasa* PGC are observed in stage 8 larvae: (1) two bilaterally symmetric cell clusters (Fig. 3m,n, $n=8$), (2) two asymmetrically positioned clusters at or near the midline (Fig. 3o, $n=11$), and (3) one cluster centered on the midline (Fig. 3p, $n=14$). *CapI-vasa* PGC expression appears to be perinuclear when viewed at 100× magnification (Fig. 3n). A single PGC cluster is visible in late stage larvae (stage 9; Fig. 3q).

CapI-vasa and *CapI-nanos* mRNA adult expression patterns

Expression of *CapI-vasa* and *CapI-nanos* was also examined in young adults 1 and 2 months after metamorphosis at different stages of sexual maturity. Generally, animals are reproductive 8–10 weeks after metamorphosis when raised at 15°C. Both *CapI-vasa* and *CapI-nanos* expression are observed in three distinct domains in adults: in the PGCs, the gonads and in the posterior growth zone (Fig. 4). Additionally, *CapI-nanos* is expressed in a small number of segmentally repeated cells in the ganglia of the ventral nerve cord and in two lateral, ectodermal patches immediately anterior to the nuchal organs (not shown). Within the thoracic region (setigers 1–9) of males, females, and hermaphrodites, *CapI-vasa* and *CapI-nanos* are expressed in a discrete non-segmental structure containing more than 50 cells, located at the ventral midline between the ventral nerve cord and the gut (Fig. 4a–d,l). This structure is clearly distinct from surrounding tissues, does not show obvious signs of cellular differentiation, and is suspended in the coelomic cavity by mesenteries (Fig. 4a,b). It is consistently localized to segment 5, usually extending into segment 6 (Fig. 4a,b). The *CapI-vasa* and *CapI-nanos*-positive cells in this structure have large nuclei and do not show overt signs of differentiation (Fig. 4d). We observed this structure in sexually immature males and females (1 month postmetamorphosis) as well as in sexually reproductive adults that contain mature gametes. To our knowledge, this structure has not been previously described in *Capitella* sp. I adults. Because of the coexpression of both *CapI-vasa* and *CapI-nanos* in cells of this midline mesodermal structure, the morphology of the cells, and its similar position to the position of the *CapI-vasa* and *CapI-nanos*-expressing PGCs in segment 4 of stage 8 larvae, we propose that this structure represents the adult PGC niche. Furthermore, we hypothesize that germ cells move from this structure into the gonads several segments posterior, where they undergo gametogenesis (Fig. 4l).

CapI-vasa and *CapI-nanos* are expressed within the ovaries of adult females. The ovaries of *Capitella* sp. I are paired ventral structures within the coelomic cavity that straddle the lateral edges of the accessory intestine and span many mid-body segments, beginning in the first abdominal segment, segment 10 (Fig. 4l; Eckelbarger et al. 1984). Each

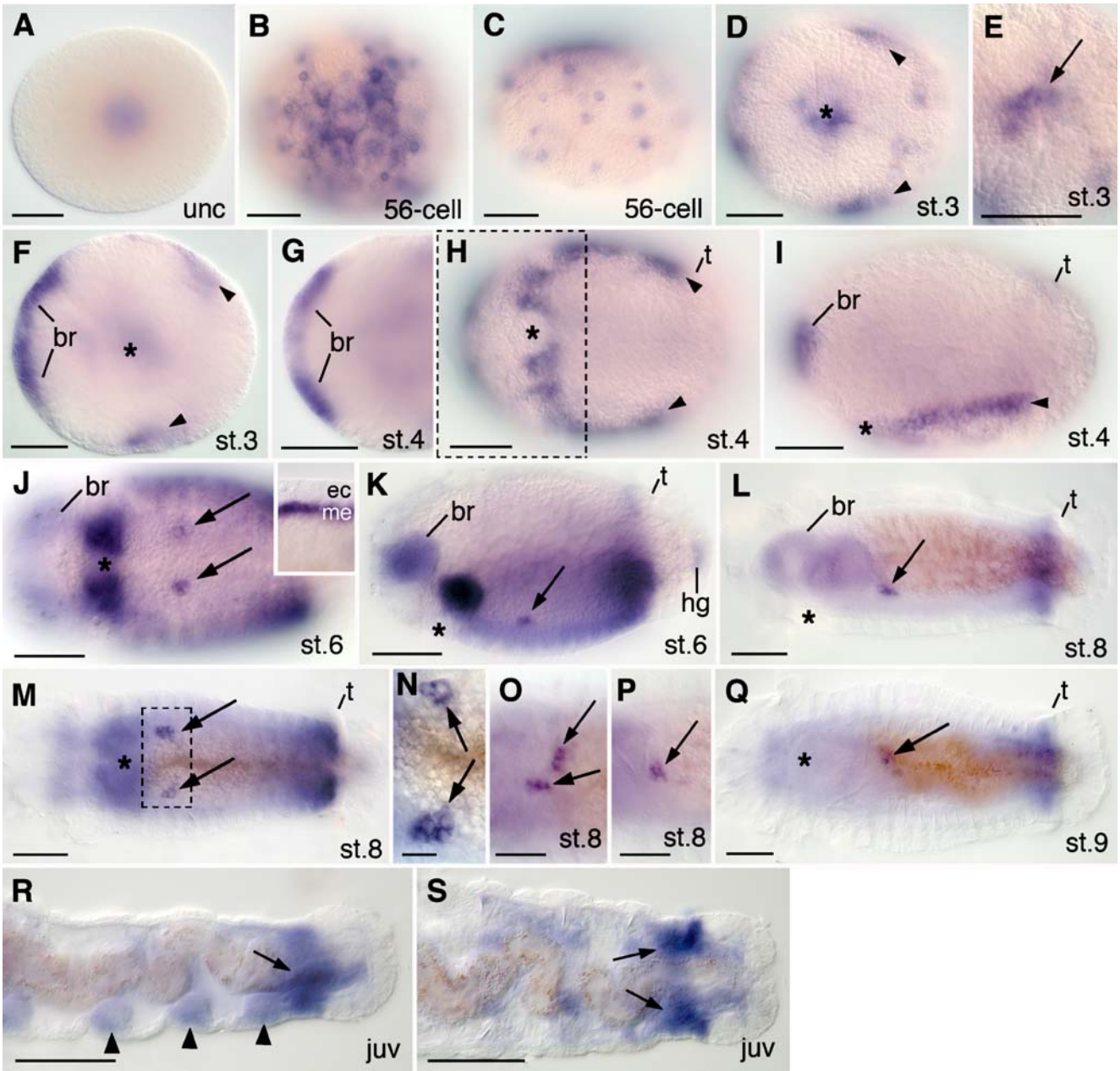

ovary contains oocytes at different stages of development (Eckelbarger et al. 1984). When examined in detail, it is clear that *CapI-vasa* and *CapI-nanos* transcripts are present in the cytoplasm of immature oocytes but are not detected in mature oocytes within the same ovary (Fig. 4e,f). Mature clusters of oocytes examined in ovaries of other animals do not express *CapI-vasa* (not shown).

In young adult males, *CapI-nanos* and *CapI-vasa* are expressed in bilateral cell clusters in a ventro-lateral position within the coelom at the junction between segments 7 and 8 and 8 and 9 (Fig. 4g and data not shown). These clusters are attached to the peritoneum, and their nuclei appear to occupy most of the area of the cell. Although *Capitella* sp. I lacks a well-defined testis, specialized proliferative zones of cells attached to the body wall between the seventh and eighth segments and in the eighth segment have been described where spermatogonia are released into the coelom (Eckelbarger and Grassle 1987b). We hypothesize that these *CapI-nanos* and *CapI-vasa*-positive cell clusters represent male gamete precursors. In more mature males (manifest by the presence of dorsal genital spines), paired genital ducts are visible at the junction of segments 7 and 8 (Eckelbarger and Grassle 1987b; Fig. 4h,l). The genital ducts are positioned dorsal to the *CapI-nanos* and *CapI-vasa*-positive cell clusters visible at the junction between segments 7 and 8 (Fig. 4h). Although the genital ducts store mature sperm,

Fig. 3 *CapI-vasa* RNA expression patterns in embryos, larvae, and juveniles. The image in **n** was captured with a 100× objective; all other images were captured with a 40× objective. Except for cleavage stages, animals are oriented anterior to the left with ventral facing down in lateral views. An *asterisk* marks the position of the blastopore (stage 3) or stomodeum (stages 4–9), *t* indicates the position of the telotroch, and *br* indicates the brain in panels where these structures are in view. **a** In the uncleaved zygote (*unc*), *CapI-vasa* RNA is detected in the yolk-free cytoplasm. **b** In animal view at 56-cell stage (fifth to sixth cleavages), cytoplasmic and nuclear staining is detected in most if not all micromeres. **c** An equatorial view (vegetal down) shows *CapI-vasa* staining in vegetal macromeres and in first through fourth quartet micromeres. **d** A ventral view of a late gastrula (stage 3) embryo shows *CapI-vasa* expression around the closing blastopore and at the position of the mesoderm 4d descendants (*arrowheads*). The out of focus staining posterior to the 4d descendants is transcript localized to the nucleus in a small number of unknown cells. **e** shows a close-up lateral view of *CapI-vasa* expression in the mesoderm cells (area depicted by *arrowhead* in **d**. **f** A dorsally mounted stage 3 embryo shows clear presumptive brain expression. *Arrowheads* point to *CapI-vasa* expression in the mesoderm cells. Stage 4 ventral (**g**, **h**) and lateral (**i**) views show *CapI-vasa* expression in brain, foregut (staining lateral to the stomodeum), and mesodermal bands (*arrowheads*). Region shown in **g** is depicted by boxed areas in **h**. **j**, **k** Ventral (**j**) and lateral (**k**) view of stage 6 larvae showing *CapI-vasa* expression in the foregut (staining lateral and dorsal to the stomodeum), brain, mesoderm (*me*) of the body segments (region between the stomodeum and telotroch, *inset* in **j**), and hindgut (*hg*). *Arrows* in **j** and **k** point to two patches of *CapI-vasa*-expressing cells (putative primordial germ cells, PGCs) in segment 4. Lateral view (**k**) shows the PGCs positioned between the endoderm and the ventral nerve cord. *Ec* Ectoderm. Lateral (**l**) and ventral (**m**) views of stage 8 larvae show strong expression in the PGCs (*arrows*) and posterior growth zone (staining anterior of the telotroch). **n** The PGCs in **l** were viewed at 100× magnification to show the perinuclear pattern of *CapI-vasa* expression. (**n**, **o**, **p** ventral views, cropped views of *boxed region* in **m**). Three distinct patterns of *CapI-vasa* PGC expression are observed among stage 8 larvae: (1) two bilaterally symmetric cell clusters (**m**, **n**), (2) two clusters positioned asymmetrically near or at the midline (**o**), and (3) one cluster at the midline (**p**). **q** At stage 9, *CapI-vasa* is expressed in the posterior growth zone and in the PGCs (*arrow*; ventral view). Posterior end of a juvenile worm (*juv*) in lateral (**r**) and ventral (**s**) view shows robust *CapI-vasa* expression in the mesoderm and ectoderm of the posterior growth zone (*arrows*) and weak expression in the ventral nerve cord ganglia (*arrowheads*). *Scale bar*, 50 μm for all panels except **n**, **o**, and **p**. *Scale bar* in **n**, 10 μm, *scale bar* in **o** and **p**, 25 μm

we could not unambiguously determine whether the expression we observed in this structure was in the somatic tissue of the coelomoduct or in sperm stored within the coelomoduct. *Capitella* sp. I also exhibits hermaphroditism (Petraitis 1985), and in these animals, *CapI-nanos* and *CapI-vasa* is expressed in maturing oocytes as well as in the ventro-lateral clusters at the junction of segments 7 and 8 and 8 and 9 (not shown). Expression of *CapI-nanos* and *CapI-vasa* in both male and female gametes contrasts with expression of these genes in *Platynereis*, in which expression of *vasa* is only observed in female gametes (Rebscher et al. 2007).

Expression of *CapI-nanos* and *CapI-vasa* in the posterior end of adults is very similar for both genes and includes ectodermal and mesodermal cells of the posterior growth zone (Fig. 4i) and ectodermal cell clusters lateral to the ganglia of the ventral nerve cord in newly formed posterior segments (Fig. 4j,k).

Comparisons of *CapI-vasa* and *CapI-nanos* expression patterns

Our whole-mount in situ hybridization studies demonstrate that *CapI-nanos* and *CapI-vasa* show largely overlapping expression patterns during embryonic, larval, juvenile, and adult stages, although *CapI-nanos* has a broader expression profile at several life history stages. Within the same cells, nuclear localization of *CapI-nanos* during cleavage and gastrulation stages is quite distinct from cytoplasmic distribution of *CapI-vasa*. *CapI-vasa* and *CapI-nanos* exhibit both somatic and germ line expression; thus, in *Capitella* sp. I, neither transcript is restricted to the germ line. The expression patterns observed at earlier stages are quite broad and include many tissues, although by late larval stages, robust expression of *CapI-nanos* and *CapI-vasa* is restricted to the PGCs and the posterior growth zone. A similar progression of expression patterns (broad somatic expression followed by more restricted expression in PGCs) has recently been described for a *vasa* orthologue in *P. dumerilii* (Rebscher et al. 2007; Zelada-González 2005), and in the oligochaete *T. tubifex* (Oyama and Shimizu 2007).

Overlapping perinuclear expression of both *CapI-nanos* and *CapI-vasa* in ventro-lateral clusters of cells at larval stages 6–8 identifies a population of putative PGCs. Although early expression of *CapI-nanos* and *CapI-vasa* in the PGCs is downregulated long before there is evidence of germ line differentiation, re-expression in the PGCs at the same location and in the gonads is apparent in young adults. Analysis of *CapI-nanos* and *CapI-vasa* expression in the PGCs and gonads has led us to the following testable hypothesis concerning the origin and development of PGCs in *Capitella* sp. I. The PGCs arise from the mesodermal precursor cell, 4d, and are visible in segment 4 as bilateral clusters of three to six cells each at larval stage 6. These two clusters converge at the ventral midline to become a single PGC cluster during late larval stages (stage 8). In young adults, the PGC clusters proliferate, resulting in a large cluster of more than 50 cells in sexually mature adults. From larval to adult stages, the PGCs move posterior by one segment, from segment 4 to 5. PGCs migrate from this large cluster to the appropriate gonad where they undergo gametogenesis. *Capitella* sp. I maintains a population of PGCs in sexually mature adults, which can respond to environmental stimuli to induce hermaphroditism. Maintenance of PGCs in sexually mature adults also serves as a store for the generation of multiple broods per individual or to populate regenerating ovaries. Future cell lineage studies will be needed to unambiguously determine if the cells we

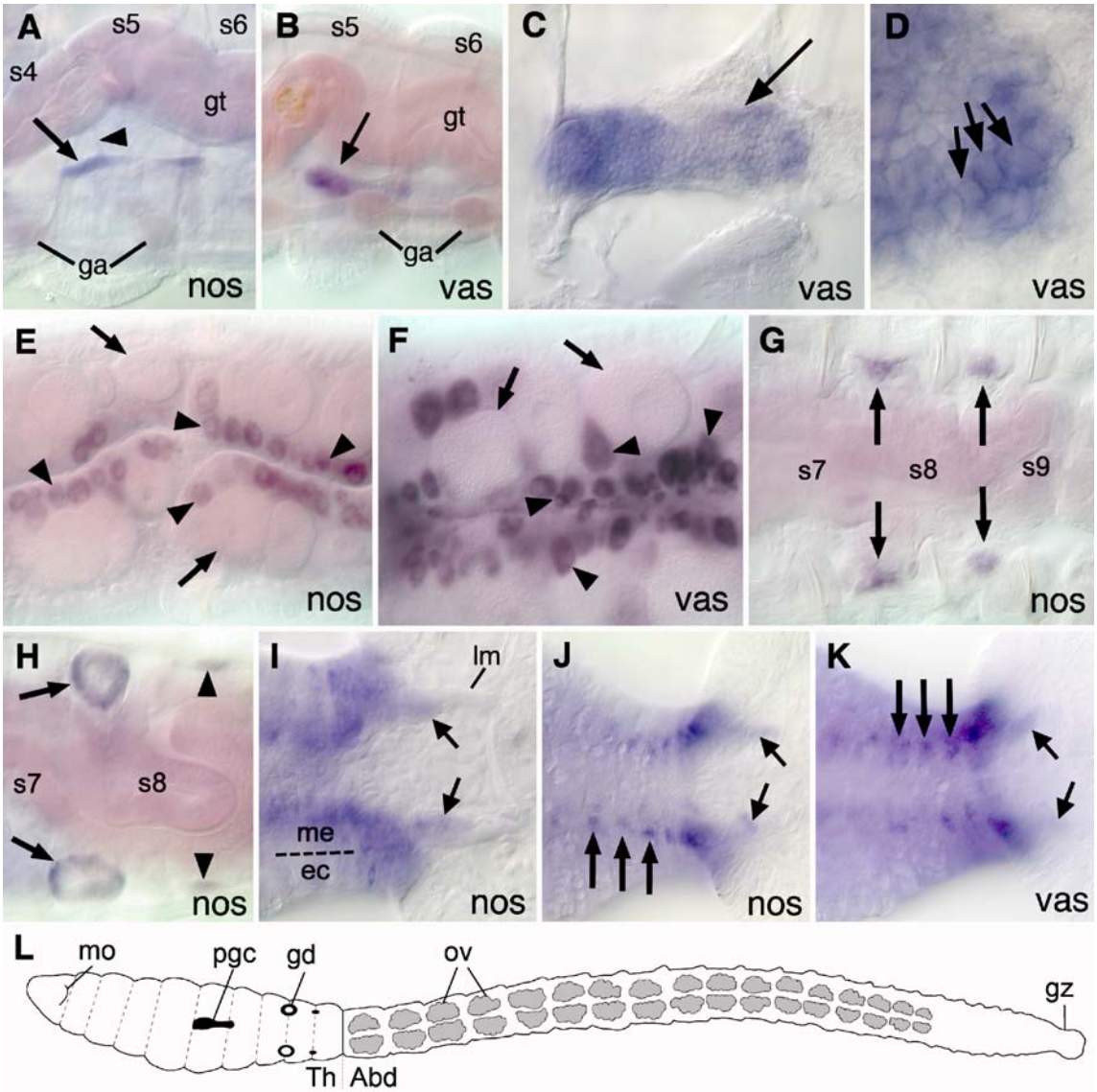

Fig. 4 Adult expression of *CapI-vasa* and *CapI-nanos*. For all panels, animals are oriented anterior to the left with ventral facing down in lateral views. **a** Close-up lateral view of segments 4–6 (*s4–s6*) showing *CapI-nanos* expression in a structure within the coelomic cavity (*arrow*), between the gut (*gt*) and ganglia (*ga*) of the ventral nerve cord in segments 5 and 6. *Arrowhead* points to mesentery attached to the gut and *CapI-nanos*-expressing structure. **b** *CapI-vasa* is expressed in cells of a mesodermal structure (*arrow*), positioned between the ganglia of the ventral nerve cord (*ga*) and the gut (*gt*) in segments 5 and 6 (lateral view). **c** Enlarged dorsal view showing *CapI-vasa* expression in the mesodermal structure positioned at the midline of segment 5 (*arrow*). In this specimen, the midline of the dorsal body wall was cut and the gut removed for better imaging. **d** Enlarged view of region of **c** (100×) showing cellular detail of *CapI-vasa*-positive cells, which have large nuclei as determined by the nuclear stain Hoechst (not shown). *Arrows* point to three *CapI-vasa*-positive cells. **e** Within the ovaries, *CapI-nanos* is expressed in immature oocytes (*arrowheads*) but is absent from mature oocytes (*arrows*), ventral view. **f** Ventral view of ovaries showing cytoplasmic expression of *CapI-vasa* in immature oocytes (*arrowheads*). *Arrows* point to mature oocytes that lack *vasa* expression. **g** Young adult males show *CapI-nanos* expression in two bilaterally symmetric mesodermal clusters (*arrows*) in a ventro-lateral position at the junction between segments 7 and 8 (*s7*, *s8*) and segments 8 and 9 (*s8*, *s9*). Ventral view. **h** *Arrows* point to *CapI-nanos*-positive genital ducts between segments 7 and 8 (*s7*, *s8*) in males. Weak *CapI-nanos* mesodermal expression is at the junction between segments 8 and 9 (*arrowheads*), ventral view. **i** *CapI-nanos* is expressed in both the ectoderm (*ec*) and mesoderm (*me*) in the posterior growth zone (ventral view). Mesodermal expression extends posteriorly along the medial edge of a longitudinal muscle (*lm*) into the pygidium (*arrows*). **j** Surface ventral view showing *CapI-nanos* expression in segmentally iterated ectodermal cell clusters immediately lateral to the ganglia of the ventral nerve cord in newly forming segments at the posterior end of the animal (*vertical arrows*). *Diagonal arrows* point to mesodermal expression in the pygidium. **k** *CapI-vasa* is expressed in the mesoderm of the posterior growth zone (*diagonal arrows*) and in newly formed segments, ventral view. *Vertical arrows* point to segmentally iterated ectodermal cell clusters positioned lateral to the ventral ganglia. **l** Schematic of adult hermaphrodite showing position of structures highlighted in **a**–**k**, ventral view. The distinct thoracic (*Th*) and abdominal (*Abd*) body regions are marked. *mo* Mouth, *pgc* putative primordial germ cells, *gd* genital ducts, *ov* ovary, *gz* growth zone, *Nos nanos*, *vas vasa*

have identified as PGCs arise from 4d and eventually give rise to germ cells.

Acknowledgments The *Capitella* sp. I genomic and EST sequence data were produced by the US Department of Energy Joint Genome Institute (http://www.jgi.doe.gov). We thank David Lambert for sending preprints prior to publication and Olivia Veatch for optimizing the adult in situ hybridization conditions. We gratefully acknowledge valuable comments on the manuscript from Michael Boyle, Neva Meyer, Kevin Pang, and Olivia Veatch. This work was supported by the National Science Foundation (IOB05-44869).

References

Curtis D, Treiber DK, Tao F, Zamore PD, Williamson JR, Lehmann R (1997) A CCHC metal-binding domain in Nanos is essential for translational regulation. EMBO J 16:834–843

Eckelbarger KJ (1984) Comparative aspects of oogenesis in polychaetes. Gustav Fischer, Stuttgart

Eckelbarger KJ, Grassle JP (1983) Ultrastructural differences in the eggs and ovarian follicle cells of *Capitella* (Polychaeta) sibling species. Biol Bull 165:379–393

Eckelbarger KJ, Grassle JP (1987a) Interspecific variation in genital spine, sperm, and larval morphohlogy in six sibling species of *Capitella*. Bull Biol Soc Wash 7:62–76

Eckelbarger KJ, Grassle JP (1987b) Spermatogenesis, sperm storage and comparative sperm morphology in nine species of *Capitella*, *Capitomastus* and *Capitellides* (Polychaeta: Capitellidae). Mar Biol 95:415–429

Eckelbarger KJ, Linley PA, Grassle JP (1984) Role of ovarian follicle cells in vitellogenesis and oocyte resorption in *Capitella* sp. I (Polychaeta). Mar Biol 79:133–144

Extavour CG, Akam M (2003) Mechanisms of germ cell specification across the metazoans: epigenesis and preformation. Development 130:5869–5884

Extavour CG, Pang K, Matus DQ, Martindale MQ (2005) vasa and nanos expression patterns in a sea anemone and the evolution of bilaterian germ cell specification mechanisms. Evol Dev 7:201–215

Grassle JP, Grassle JF (1976) Sibling species in the marine polution indicator *Capitella* (Polychaeta). Science 192:567–569

Holbrook MJL, Grassle JP (1984) The effect of low density on the development of simultaneous hermaphoroditism in male *Capitella* species I (Polychaeta). Biol Bull 166:103–109

Kang D, Pilon M, Weisblat DA (2002) Maternal and zygotic expression of a nanos-class gene in the leech *Helobdella robusta*: primordial germ cells arise from segmental mesoderm. Dev Biol 245:28–41

Kimble JE, White JG (1981) On the control of germ cell development in *Caenorhabditis elegans*. Dev Biol 81:208–219

Lawson KA, Hage WJ (1994) Clonal analysis of the origin of primordial germ cells in the mouse. Ciba Found Symp 182:68–84 discussion 84–91

Meyer, N.P. and Seaver, E.C. Mechanisms of neurogenesis in an annelid: characterizing neural progenitors in *Capitella* sp. I. (in preparation)

Mochizuki K, Nishimiya-Fujisawa C, Fujisawa T (2001) Universal occurrence of the vasa-related genes among metazoans and their germline expression in Hydra. Dev Genes Evol 211:299–308

Nieuwkoop PD (1947) Experimental observations on the origin and determination of germ cells, and on the development of the lateral plates and germ ridges in the urodeles. Arch Neerl Zool 8:1–205

Oyama A, Shimizu T (2007) Transient occurrence of vasa-expressing cells in nongenital segments during embryonic development in the annelid *Tubifex tubifex*. Dev Genes Evol 217:675–690

Petraitis P (1985) Females inhibit males' propensity to develop into simultaneous hermaphrodites in *Capitella* sp. I (Polychaeta). Biol Bull 168:395–402

Pilon M, Weisblat DA (1997) A nanos homolog in leech. Development 124:1771–1780

Rabinowitz JS, Chan XY, Kingsley EP, Lambert JD (2008) Nanos is required in somatic blast cell lineages in the posterior of a mollusc embryo. Curr Biol 18:331–336

Rebscher N, Zelada-González F, Banisch TU, Raible F, Arendt D (2007) Vasa unveils a common origin of germ cells and of somatic stem cells from the posterior growth zone in the polychaete *Platynereis dumerilii*. Dev Biol 306:599–611

Ronquist F, Huelsenbeck JP (2003) MrBayes 3: Bayesian phylogenetic inference under mixed models. Bioinformatics 19:1572–1574

Seaver EC, Kaneshige LM (2006) Expression of 'segmentation' genes during larval and juvenile development in the polychaetes *Capitella* sp. I and *H. elegans*. Dev Biol 289:179–194

Seaver EC, Paulson DA, Irvine SQ, Martindale MQ (2001) The spatial and temporal expression of Ch-en, the engrailed gene in the polychaete *Chaetopterus*, does not support a role in body axis segmentation. Dev Biol 236:195–209

Seaver EC, Thamm K, Hill SD (2005) Growth patterns during segmentation in the two polychaete annelids, *Capitella* sp. I and *Hydroides elegans*: comparisons at distinct life history stages. Evol Dev 7:312–326

Swartz SZ, Chan XY, Lambert JD (2008) Localization of Vasa mRNA during early cleavage of the snail *Ilyanassa*. Dev Genes Evol 218: 107–113

Swofford DL (2002) Phylogenetic analysis using parsimony (*and other methods). Sinauer, Sunderland, MA

Takamura K, Fujimura M, Yamaguchi Y (2002) Primordial germ cells originate from the endodermal strand cells in the ascidian *Ciona intestinalis*. Dev Genes Evol 212:11–18

Tam PP, Zhou SX (1996) The allocation of epiblast cells to ectodermal and germ-line lineages is influenced by the position of the cells in the gastrulating mouse embryo. Dev Biol 178:124–132

Williamson A, Lehmann R (1996) Germ cell development in *Drosophila*. Annu Rev Cell Dev Biol 12:365–391

Yoon C, Kawakami K, Hopkins N (1997) Zebrafish vasa homologue RNA is localized to the cleavage planes of 2- and 4-cell-stage embryos and is expressed in the primordial germ cells. Development 124:3157–3165

Zelada-González F (2005) Germline development in *Platynereis dumerilii* and its connection to embryonic patterning. Combined Faculties for Natural Sciences and for Mathematics. Ruperto-Carola University of Heidelberg, Heidelberg, p 175